Petrophysical and Petrographic Analysis of the PBF-10 Cores

Selected intervals between 969 and 1172 feet were cored in the PBF-10 well. Fifty-five thin sections were made from the cores. The thin sections were tescribed and photographed. Each thin section was impregnated with blue epoxy, so porosity is blue in the photomicrographs. Half of each thin section was stained with Alizarin Red, which turns calcite red.

Based on the rock classification and fossil content, each thin section was assigned a lithofacies. Twelve lithofacies were identified: sandy mollusk packstone, algal boundstone, algal coated-grain packstone, sandy echinoid packstone, sandy echinoid coated-grain packstone, very fine-fine grained dolomitic fossiliferous sandstone, skeletal wackestone, very fine grained dolomitic fossiliferous sandstone, foram pellet packstone, intraclastic pellet packstone, wackestone, and algal packstone.

Based on the porosity and permeability (core analysis and thin section descriptions) of each thin section, petrophysical facies were assigned. The thin sections group naturally into five categories and have a high correlation with the porosity and permeability logs.

The petrophysical facies are as follows:

Key to Petrophysical Facies
Based on Core Analysis

Petrophysical Facies #1: Low porosity, low permeability (isolated moldic porosity)

Petrophysical Facies #2: High porosity, high permeability (connected moldic porosity)

Petrophysical Facies #3: High porosity, low permeability (sandstone with small interparticle porosity)

Petrophysical Facies #4: Very high porosity, very high permeability (well connected, vuggy and interparticle porosity)

Petrophysical Facies #: Very high porosity, very low permeability (isolated moldic, interparticle, and intraparticle porosity)

The enclosed report includes photographs of the slabbed cores. Porosity and permeability values, along with the petrophysical facies, are noted on the photos. Each photomicrograph includes permeability and porosity logs and descriptions of the lithofacies and petrophysical facies.

Hughbert Collier
September 7, 2001

NMR and acoustic signatures in vuggy carbonates of South Florida

J.O. Parra, C.L. Hackert, Southwest Research Institute; H.A. Collier, Collier Consulting; and M. Bennett, South Florida Water Management District

Summary

Digital processing of optical macroscopic (OM) , SEM and X-ray computed tomography (CT) images, and petrography characterize the pore space of the pore system of vuggy carbonates in South Florida. The results of this analysis provided supportive information to evaluate NMR well log signatures for NMR well log calibration. Saturated and desaturated NMR core measurements estimated the irreducible water in the rock (associated with the matrix porosity) and estimate the variable T2 cut offs for the NMR well log calibration. The measurements established empirical equations to extract permeability from NMR well logs in South Florida. Analysis of synthetic and observed NMR signatures demonstrated that NMR well logs capture only the micro and macro porosities of the carbonate rock. The CT image processing and the ultrasonic analysis provided information to characterize the acoustic signatures caused by interconnected and connected vugs in core samples. The ultrasonic core and geotechnical data provided velocity versus porosity relationships based on flow zone indicators. This relationships are input in a poroelastic modeling program to determine the squirt flow lengths associated with the fluid flow between the matrix and the vugs and between the vugs. Based on this information attenuation and dispersion curves of the vuggy carbonate rock are simulated in the frequency range of sonic logs. This suggests that full waveform sonic can image the vuggy carbonate rock.

Introduction

The objective of this study is demonstrate how NMR and acoustic techniques can complement each other to characterize vuggy carbonate formations. To accomplish our objective we use core and well log data from well PF10 that intercepts a fresh-water aquifer of the Ocala Group unit in Palm Beach, South Florida.

The carbonate rock in South Florida, and carbonate formations in general have broad pore size distributions, from microcrystalline to large vugs. These pore spaces and their geometries are crucial factors to understand the applications that include hydrocarbon reservoir characterization, hydrological and environmental issues. In many regions carbonates form aquifers and the understanding of their pore systems are critical for the hydrological process. The pore system of carbonates have been recognized to be physically and genetically complicated by Choquette and Pray (1970) who published a review on the geological nomenclature and the classification of carbonates, and introduced terminology that emphasizes interrelations between porosity and other geological features. In Choquette and Pray's review seven dominant porosity types in sedimentary carbonates were considered. These porosity types are inter particle, intra particle, inter crystal, moldic, fenestral, vug and fracture. The Ocala group in South Florida

1

contains all these type of porosity except fracture porosity. In particular vugs are the most important porosity that are forming the pore structure. In most of the cores the vugs are recognized visually; there are separated vugs and touching vugs observed in the cores. Touching-vug pore geometries usually consist of interconnected large cavities, and channels (see Choquette and Pray , 1970). The typical vug diameter is about 16 mm in cores from well PF10. The vugs are longer in the vertical direction than the horizontal direction

Lucia (1983) showed that the most useful division of pore types for petrophysical purpose was of pore space between grains or crystals, called inter particle porosity and all other pore space, called vuggy porosity. The vuggy pore space was further subdivided by Lucia(1983) into two groups depending how the vugs are interconnected: (1)   Vugs interconnected only through the interparticle pore network are separate vugs, and (2) vugs that form an interconnected pore system are touching vugs. The work by Lucia is the concept that pore-size distribution controls permeability and saturation and that pore-size distribution is related to rock fabric.

Anselmetti et al. (1998) describes a method of characterization of carbonate samples based on quantitative observations from digital environmental SEM (ESEM) and optical microscopic (OM)   thin section images. This approach has the advantage of avoiding descriptive bias by the geologist, but also has a disadvantage in that quantitative data obtained by image analysis are dependent on thin-section selection and field of view under the microscope.

In this paper we include thin section/SEM and x-ray computed tomography (CT) data to characterize the carbonate pore space with size varying by more than five orders of magnitude in the sample space. The CT method produces 3 D images of the pore structure by giving a visualization to the vugs present in the core sample. In addition, we use NMR core measurements to produce T2 distribution based on saturated and desaturated samples. These data provide capillary-bounded water in the core and it can provide pore size distributions from core samples. Several measurements are made to apply the relaxivity grouping technique to estimate the T2 cut- offs for well log calibration in carbonates. The thin section/SEM image analysis is used to confirm quantitatively/qualitatively the expect relation between NMR T2 signatures and pore size distributions. Thus the objective of the thin section/SEM and CT image analysis as well as the core data is to provide supporting information to evaluate the variable T2 cut-off method to calibrate NMR well logs for extracting porosity and permeability to characterize vuggy carbonates.

In addition, our approach includes ultrosonic and full waveform sonic to evaluate whether the vuggy porosity can be characterized and detected in the region surrounding the borehole with sonic tools. Based on standard core measurements and image analyses, we constructed vuggy porosity models to calculate synthetic ultrasonic responses based on the finite difference method, and we compared the synthetic with ultrasonic data. We used the modeling results to explain the scattering of velocity versus permeability relations based on core measurements for different flow units of the carbonate aquifer. To determine whether we can assess the degree of connectivity between vugs or between the matrix and the vugs based on acoustic data, we calculated the squirt-flow lengths using poroelasticity (Parra, 2000). In addition, we calculate dispersion and attenuation curves based on core data in the frequency range of sonic logs to determine whether P-wave attenuation can be related to the fluid flow between the matrix and the vugs and to establish the application of sonic logs for estimating whether vugs contribute to permeability in

2

the region surrounding the borehole.

Pore and Core Scale Images

We have selected two core samples with vuggy porosity. We analyzed the carbonate rock samples at the pore and core scales by including imaging processing of thin section, SEM and CT data. CT images from cores #7 and # 41 are processed and analyzed to measure the vuggs size distributions. The images are modeled to simulate ultrasonic waveforms to analyze the effects of saturated and unsaturated vuggy core samples on the compressional wave velocity. The optimal application is to devise methods to characterize vuggs at the core and borehole scales based on acoustic and ultrasonic measurements.

Optical macroscopic (OM) thin sections, and SEM images are from samples selected from cores #7 and #41. The type of minerals and porosity is provided by the petrography analysis of the thin sections The analysis of the SEM and OM images provide information on the pore sizes of the rock matrix, which is used to calculate synthetic T2 distribution to evaluate the NMR well log signatures. Since the SEM/OM images can give a good indication whether the micro and /or the macro porous are connected, then a more accurate T2 cut offs can be determined to calibrate the NMR well logs. In general the image analysis helps to characterize the pore structure of the carbonate rock. In the present study NMR well logs supported with thin sections and core images defines the matrix porosity of the carbonate rock, and the acoustic data with core data detects vuggy porosity of carbonate formation surrounding the borehole.

Thin Section and SEM photomicrographs

We have conducted thin section petrography and scanning electron microscopy (SEM) of two carbonate samples Core # 7 and Core # 4l. The objective is to; 1) provide petrographic descriptions of rock texture, fabric and mineralogy and 2) describe the pore system properties. Both of the samples analyzed are carbonates, although their textures are quite different. The sample # 7 is a grainstone , while the sample # 41) is a wackestone .

The skeletal grainstone exhibits the greatest diversity of acrboante allochems, including echinoderms, milliolid and rotalid forams, work tubes, pelecypods, perloids, intraclasts, various algal grains, gastropods, bryozoans, and ostracodes. Additional, upper very fine to lower fine-grained quartz and feldspar sand is distributed throughout the sample in moderate amounts. The skeletal assemblage, grain size and shortage of carbonate mud are indicative of high energy sedimentation in a normal marine environment. In contrast, the wackestone sample contains a less diverse assemblage of framework grains, which includes forams, ostracodes, peloids, intraclasts, algal grains and corals. Also in contrast to the grainstone sample is the abundance of carbonate mud. This wakestone low energy, normal marine sedimentation.

The pore system of skeletal grainstone comprise moldic, vuggy, intergranular, interparticle and inercrystalline pores;visible porosity is approximately 17 % by point count. Additional, microporos associated with micritic grains such as peloids and intraclasts are present in minor amounts; however, they do not contribute to the effective pore volume. Syntaxial overgrowths and fringing and equant calcite cements are the most abundant pore-filling constituents in this

3

sample; dead oil is locally present.

Very little primary porosity is present in the wackestone sample. Moldic and vuggy pores dominate the assemblage of visible pores, with fewer inter crystalline and intra particle pores. Total visible porosity was determined to be approximately 8 % by point count. Microporous are common in the micritic matrix and contribute significantly to the total porosity to the wackestone sample. However, despite their large contribution to the total pore volume, these micropores do not contribute to the effective pore volume or permeability of this sample.

Core imaging and relation to NMR T2 distribution

NMR T_2 distributions are commonly associated with pore size. This is the basis underlying NMR logging for permeability, as larger pores are assumed to be indicative of higher permeability formations. .

We begin with pore imaging from three different techniques, spanning a range of length scales. The first method, x-ray computed tomography (CT), produces three-dimensional images of whole cores with a pixel resolution of about 0.25 mm. This is primarily useful for imaging vugs. The second technique is optical microscopy (OM) of thin sections, which provides a pixel resolution on the order of 2 μm. This is useful for imaging moldic and interparticle porosity. The third technique is scanning electron microscopy (SEM) on polished core fragments, which we use to image microporosity with a pixel resolution of 30-300 nm.

To obtain the pore size and shape distribution from these images, we follow the method of Anselmetti et al. (1998) and use public domain software developed by NIH and Scion Corp. called Scion Image™. The first step is to convert the core images to TIF format grayscale files, where black represents pore space and white represents matrix. A macro written for the Scion Image program then cleans the image to eliminate single pixel noise, thresholds the image to divide pore from matrix, counts the pores, and determines the area, perimeter, and shape factor for each pore. These results may then be saved to a file.

A postprocessing program computes the pore radius and histograms of pore radius distribution. The pore radius is taken to be

$$r_{pore} = 2\left(\frac{area}{perimeter}\right), \qquad (1)$$

as this gives the length scale associated with the narrower axis of elliptical shaped pores. It is the narrow axis which controls the NMR T_2 relaxivity response. This response is typically expressed as

$$\frac{1}{T_2} = \frac{2\rho}{r_{pore}} + \frac{1}{T_{2b}}, \qquad (2)$$

where we assume that the ratio of volume to surface area is $r_{pore}/2$. The quantity ρ is the surface

4

relaxivity, and represents the tendency for molecules to relax their magnetization at the pore wall. Values usually range from 1 to 10 μm/s in carbonates (Chang et al., 1997; Ramakrishnan et al., 1999). The quantity T_{2b} is the bulk relaxivity, and represents the time scale over which the magnetization is lost in a bulk (unbounded) fluid. In practice, workers almost always assume the bulk relaxation term is negligible compared to the surface relaxation term. However, in the Florida vuggy carbonates this assumption is unwarranted. Based on the data, it appears that the T2b bulk relaxation time is around one second.

We can demonstrate the importance of the bulk term through simple analysis using equation (2). If the surface relaxivity rate is 5 μm/s, then a pore with radius 10 μm has a T2 relaxation time of 1 second. This is a fairly small pore, but is already close to the bulk relaxation time. We know from examination of the core images that a significant fraction of the Florida carbonate porosity is in larger moldic and vuggy porosity, but this would not be apparent from the NMR logs. It may be argued that large pores do not contribute much to the formation permeability, and so it doesn't matter if the NMR log distinguishes them from smaller pores. An examination of the NMR log, however, might lead one to the erroneous conclusion that most of the porosity is in 10-20 μm pores. In consideration of this issue, Chang et al. (1997) recommended not using T2 larger than 750 ms when computing permeability in carbonates.

Results: core 41

Core 41 is from 1138 ft depth, in an interval with a high degree of moldic and vuggy porosity. In examining this core, we used CT imaging with 0.25 mm resolution, OM with 40x magnification, and SEM with 300x and 3000x magnification. We have extracted the pore size and shape distribution from the images, and the pore size histogram is shown in Figure 1. The two SEM magnifications and the OM image have overlapping scales of view, so there is a continuous distribution of pore sizes up from 0.02 μm up to 50 μm. However, there is a gap in coverage between the largest pores observed by OM and the smallest pores observable by CT imaging. This is complicated by the fact that the smallest pores at each magnification are poorly resolved, while the largest pores are few in number. Thus, the accuracy of the pore size distribution falls off near the ends of the range of each technique. The overlapping coverage provided by the two SEM and OM magnifications is thus very valuable.

Table 1: Approximate breakdown of porosity by imaging method and porosity type
CT (vuggy) = 13% ; OM (macro) = 4% and SEM (micro) = 17%
total porosity from imaging = 33%* ; porosity from core = 32%; and
porosity from well log = 39%
*Numbers do not add exactly because of overlap in SEM and OM length scales.

From the pore size distribution, we can predict the T2 distribution. Matching the peaks of the pore size histogram and the well log T2 distribution suggests that the formation relaxivity is near 1.5 μm/s. This is within the range of acceptable values for carbonates. Figure 2 shows the predicted T2 distribution from the core in the absence of any bulk relaxation. Obviously, in this case about half of the porosity is distributed at T2 decay times much longer that those recorded by the tool. Including bulk relaxation moves the large pores to a T2 of around 800 ms, where it

5

accounts for most of the deficit between the well log T2 curve and the core T2 curve between 200 and 1000 ms.

Results: core 7

Core 7 is from 1022 ft depth, in an interval which is transitioning between sandy limestones with few moldic pores and moldic, non-sandy limestones. Thin section images of core 7 show isolated sand grains in the limestone matrix. As in core 41, we used CT imaging with 0.25 mm resolution, OM with 40x magnification, and SEM with 300x and 3000x magnification. We have extracted the pore size and shape distribution from the images, and the pore size histogram is shown in Figure 3. The comments made in the discussion of core 41 regarding scales of view also apply here.

Table 2: Approximate breakdown of porosity by imaging method and porosity type
CT (vuggy) = 4%; OM (macro) = 3%; and SEM (micro) = 12%
total porosity from imaging = 19%* ; porosity from core = 17% ; and porosity from NMR well
log = 24%
*Numbers do not add exactly because of overlap in SEM and OM length scales.

From the pore size distribution, we can predict the T2 distribution. Matching the peaks of the pore size histogram and the well log T2 distribution suggests that the formation relaxivity is near 5 μm/s, within the range of acceptable values for carbonates. The presence of sand is expected to increase the relaxivity somewhat (compared to core #41), as sandstones have higher relaxivities than carbonates. Figure 4 shows the predicted T2 distribution from the core in the absence of any bulk relaxation using a relaxivity of 5 μm/s. In this case, the 32 ms peak from the well log reflects the matrix microporosity observed in the SEM images and bulk relaxation in larger pores accounting for the 0.5 second peak.

NMR Well Log Calibration

NMR well logs from the Florida aquifer are calibrated for permeability by using a variable T2 cutoff to predict the irreducible bound fluid volume (BVI). The BVI is converted to permeability through the FZI method of Ohen et al., 1999. Values for the variable T2 cutoff are obtained through NMR measurements on fully saturated and centrifuged cores.

The original method of computing permeability from NMR well logs using a fixed T2 cutoff of 90 ms produces unsatisfactory results in the Florida carbonate aquifer system. The primary reason for this is that the region of interest includes several varied lithological units including sandstone and carbonates with varying degrees of vuggy porosity. A more accurate method of computing permeability would take into account the variations in pore structure which occur throughout the formation. We use a variable T2 cutoff to predict the bound fluid volume (BVI). The T2 cutoffs are derived from experimental measurements on nine cores from the Florida aquifer. The cores were fully saturated with water, and then NMR measurements were

taken before and after centrifuging. By comparing the T2 distributions of the fully saturated cores and the cores with irreducible saturation, we obtain a T2 cutoff separating the pore space which participates in fluid migration from the non-participating pore space. The nine cores examined so far appear to naturally separate into three relaxivity groups, based on the product of the NMR surface relaxivity and the surface area to volume ratio of the pore space. The three relaxation groups from the nine samples are obtained by plotting log T2 versus the normalized porosity ϕ_z, equal to $\phi/(1-\phi)$ and by fitting the following equation

$$\log T2 = \log (\phi_z) + \log [1/(\rho\ S_{gv})].\qquad(3)$$

This Equation classifies samples that exhibit similar NMR relaxation (rock-fluid interaction) characteristics into a group. The average parameters for the group serve as calibration points for interpreting NMR logs. The factor $1/\rho\ S_{vg}$, often referred to as relaxivity product, represents both the relaxation power and textural attributes of the formation. Thus, if $T2_i$ is the T2 value of the median pore size, and the normalized porosity ϕ_z then the 3 groups are:.

Group	T2 cutoff	$T2_i/\phi_z$
1	128 ms	> 0.3728 s
2	85 ms	0.0729 - 0.3728 s
3	6.5	< 0.0729 s

The NMR well log is divided among these three groups by examining the median T2 value at each depth. The BVI is then computed as the porosity with associated T2 values less than the T2 cutoff for that group. Once the BVI is known, we compute the flow zone indicator value and permeability for that depth through the equations (Ohen et al., 1999)

$$FZI = \left[\frac{b\left(1 - \dfrac{BVI}{\phi}\right)}{1 + a\left(\dfrac{BVI}{\phi} - 1\right)} \right]^c \qquad(4)$$

$$k = 1014\ FZI^2\ \frac{\phi^3}{(1 - \phi)^2} \qquad(5)$$

where the parameters a, b, and c are determined from the best fit to the core permeability measurements of the same nine cores used in the NMR experiment. Based on these nine cores, the optimal values are : $a = 1.05$, $b = 0.0946$, and $c = 0.337$.

The result of using the variable T2 cutoff based on the nine cores is shown in Figure 5. The overall effect is to lower the permeability, especially from the highest permeability zones. In these regions, the permeability is reduced by one order of magnitude. Some abrupt changes in permeability are also introduced, as the T2 cutoff can vary sharply from one depth to the next.

Also, the sandstone layer from 1050-1060 feet depth is probably predicted as having too high a permeability (~50 md) with this reprocessing, although the original prediction of $k < 0.1$ md is probably too low. We expect some improvements in the permeability correlation if more cores are included in the study. Tests are now underway on an additional nine cores, which will double the amount information available. Presently, the relaxation groups 2 and 3 are based only on two core measurements each, not a statistically significant sample.

Velocity Analysis

One of our goals was to establish velocity-permeability relations grouped on the basis of flow zone indicators (FZI) on a set of 24 core samples. We applied the FZI concept given by Amaefule et al. (1993) to separate the P-wave velocity in flow units as a function of permeability. The second objective was to model the observed velocity core data using poroelasticity to determine squirt-flow lengths. The best fit between observed and calculated velocity provides the squirt-flow parameters and a better bulk modulus for each sample. To determine the squirt-flow lengths for each sample based on the Biot squirt-flow mechanism (BISQ), we used the theory given in Parra (2000). To calculate phase velocity, we used the rock physical and fluid properties of permeability, porosity, grain density, grain module, the drained Vp and Vs, fluid density, fluid velocity, and fluid viscosity. The drained Vp and Vs were calculated using Gassmman equations for fluid substitution. Thus, phase velocity data for six flow units were calculated. Figure 6 shows curves a, b, c, d, e, and f associated with six flow units (i.e., FZI = 0.7, 1.25, 2.5, 4, 8, 16). In the same scatter plot, the squirt-flow lengths for each of the calculated velocities are also included. For example, curve (a) shows an increase in squirt-flow length as permeability is increased. The large permeability correlates with large flow lengths. In the same curve, the departures of the calculated velocities from the observed velocities reveals the amount of vuggy porosity that may be present in the sample. In curve (b), the fit between observed and calculated velocities is perfect. In this case the velocity is controlled only by intrinsic effects caused by the fluid flow. In curve (c), the cluster of observed and calculated velocities between 1 and 10 Darcies suggests that scattering effects due to vuggy porosity cause the difference between observed and calculated velocities. In this curve, a squirt- flow length of 2.5 cm was predicted, which corresponds to the high permeability values. The final curve (f) shows a big difference of about 1000 ft/s between the observed and calculated velocities for core 41. In this heterogenous core, Gassmman equations may not work very well. In fact, the dry Vp and Vs parameters were overestimated using Gassmman equations.

Acoustic Well Log Analysis

The poroelastic model to calculate the P-wave velocity at 250 kHz for each flow unit curve is based on the squirt-flow mechanism. To determine the phase velocity and attenuation of the vuggy carbonate rocks in the sonic log frequency, we chose the data from cores in curve (b) of Figure 6. The attenuation curves for this flow unit are given in Figure 7. In general, the curves show strong dispersion effects caused by interactions between the rock matrix and fluid. The results of this analysis suggest a strong attenuation in the frequency range between 1000 and

15000 Hz. We also observed that the peak frequency moves toward the low frequency range as the squirt-flow length is increased. In this case the flow is associated with connectivity between the vugs and the matrix. That is, as permeability increases, attenuation becomes greater. This analysis implies that sonic logs have the potential to capture fluid flow interactions between the matrix and the vugs. Specifically, the P-wave attenuation and phase velocity will capture the degree of connectivity between the matrix porosity and the vugs or the connectivity between vugs.

Monopole and dipole sonic data were recorded in the PF10 borehole at the Florida aquifer. The objective was to extract Stoneley wave permeability from sonic logs and compare Stoneley wave permeability with NMR-derived permeability to determine which technique is more suitable to use on a regular basis to characterize the aquifer. Since the Stoneley waves are sensitive to washout zones, and the PF10 borehole has many washout zones, Stoneley wave permeability does not produce good results. However, the P-wave events are easy to identify in the microseismogram of Figure 8a. The spectra of the acoustic waveforms show the attenuation of the P-wave events associated with the vuggy porosity in the region between 1014-1024 ft (see Figure 8b). The next step in the analysis is to produce synthetics based on the core data containing vugs and compare them with the observed data to determine whether we can infer from the P-wave sonic data the degree of connectivity between vugs and between the matrix and vugs. To fully evaluate this concept we will use the NMR-derived permeability log, porosity log, the density log, the Vp and Vs logs and the lithology.

Conclusions

Image analysis and petrography characterized the pore structure of the carbonate rock. NMR well log signatures supported with thin sections and core images define the matrix porosity of the carbonate rock, and the ultrasonic data detected vuggy porosity. In particular, NMR synthetic signatures based on pore size distributions, which were determined from image processing fit very well the observed NMR well log signatures. This interpretation has produced a relaxivity of 1.5 μm/s for the wackestone sample, and 5 μm/s for the grainstone sample. These two values are acceptable values for carbonates. The presence of sands in the grainstone expected to increase the relaxivity compared to that of wackestones, as sandstones have higher relaxivities than carbonates. In addition, we found that the matrix porosity of both samples is captured by the NMR well log signatures. The vuggy porosity was not clearly identified by NMR measurements. However, connected and separated vugs were detected with ultrasonic measurements. The velocity dispersion model results based on the pore structure and core data indicated that vugs in the formation surrounding the borehole, strongly attenuate the full waveform monopole data. This suggest that NMR well log together with acoustic data can image the vuggy carbonate formation at the South Florida aquifer.

Acknowledgment

References

Amaefule, J. O., Attunbay, M.., Tia B.D., Kersey, D.G., Keelan, D.K., 1993,
Enhanced reservoir description: using core and log data to identify hydraulic (flow) units
and predict permeability in cored intervals/wells: SPE 26436, 1-16.
Anselmetti, F. S., Luthi, S.,and Eberli, G. P., 1998, Quantitative characterization of carbonate
pore systems by digital image analysis, AAPG Bulletin 82, 1815-1836.
Chang, D., Vinegar, H., Moriss, C., and Straley, C. 1997, Effective porosity, producible fluid, and
permeability in carbonates from NMR logging, Log Analyst 38, 60-72.
Choquette, P. W., and Pray, L.C., 1970, Geological nomenclature and classification of porosity in
sedimentary carbonates: AAPG Bulletin, 54, 207-250.
Lucia, F. J., 1983, Petrophysical parameters estimated from visual description of carbonate rocks:
a field classification of carbonate pore space: Journal of Petroleum Technology, 35, 626-
637.
Ohen, H. A., Enwere, P.M., Kier, J., 1999, NMR relaxivity grouping or NMR facies identification
is key to effective integration of core NMR data with wireline log: SCA-9942.
Parra, J.O., 2000, Poroelastic model to relate seismic wave attenuation and dispersion to
anisotropy: Geophysics, 65, 201-202.
Ramakrishnan, T. S., Schwartz, L. M., Fordham, E. J., Kenyon, W. E., and Wilkinson, D. J.,
1999, Forward models for nuclear magnetic resonance in carbonate rocks, Log Analyst 40,
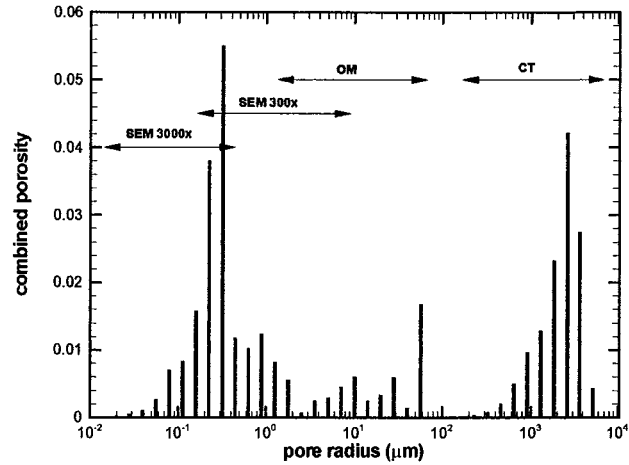260-270.

Figure 1. Pore size distribution for core # 41 based on multiple imaging methods.
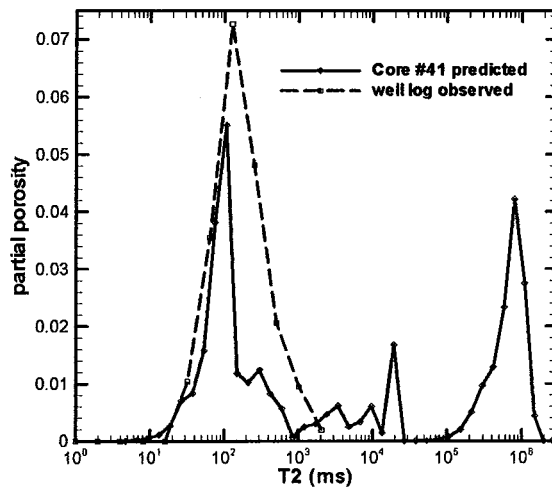

Figure 2. Predict T2 distribution based on pore size histogram of core 41, compared to T2 distribution from well log. Only the porosity measured by the SEM imaging has a T2 decay time less than the bulk rate.
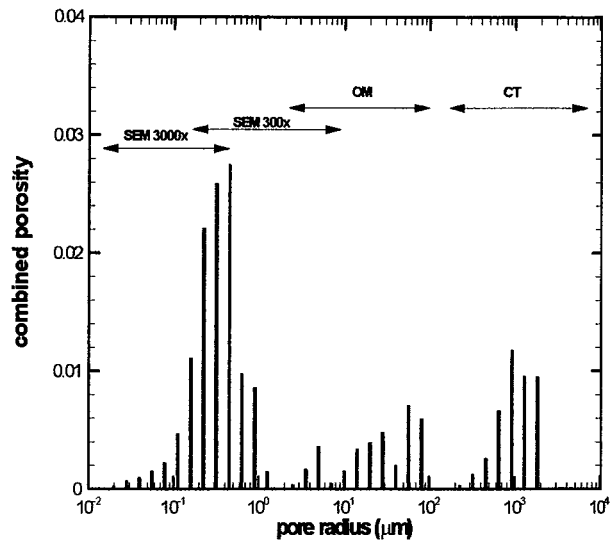
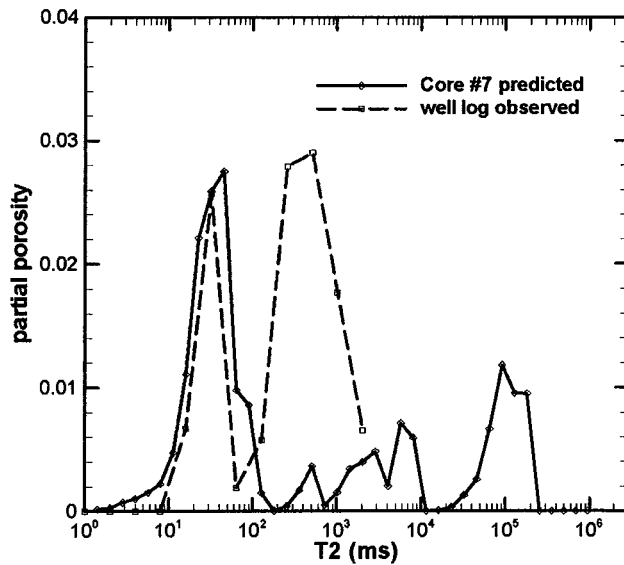Figure 3. Pore size distribution fro core #7 based on multiple imaging methods.

Figure 4. Predict T2 distribution based on pore size histogram of core 7, compared to T2 distribution from well log. Only the porosity measured by the SEM imaging has a T2 decay time less than the bulk rate.
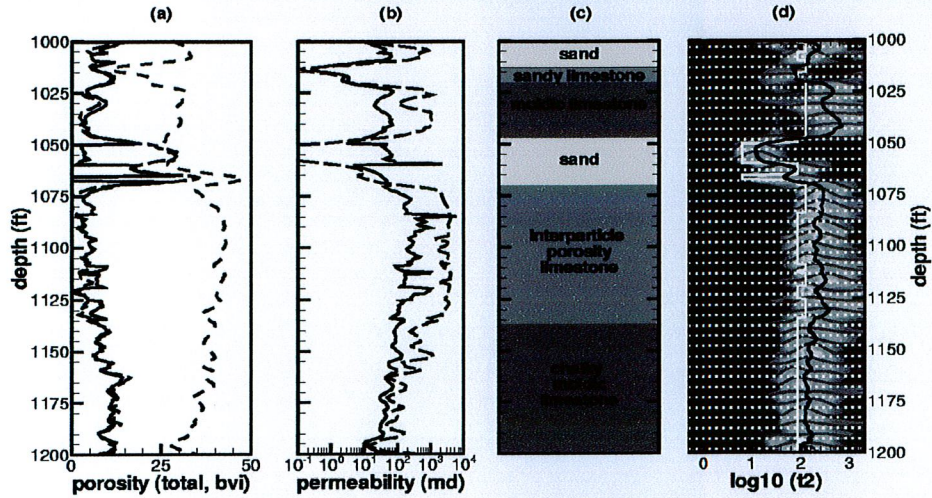
12

Figure 5. (a) Total porosity (short-dash line), standard BVI (long-dash line), and reprocess BVI (solid line);(b) standard permeability (long-dash line) and reprocessed permeability (solid line); (c) lithological units; and (d) NMR distribution with variable cutoff (white line) and media T2 (black line).
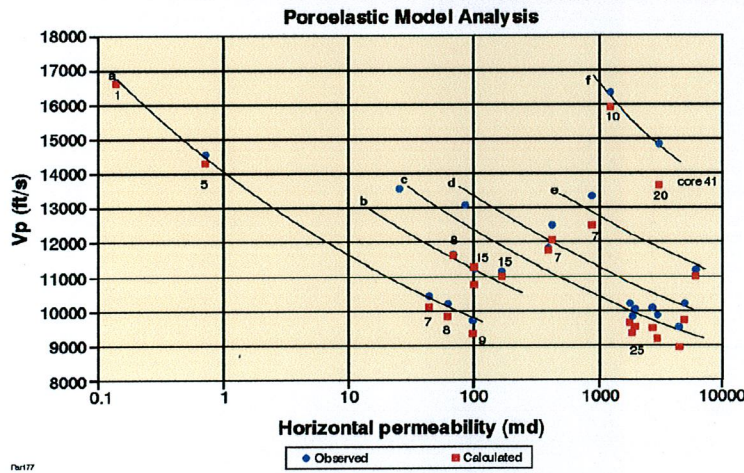

Figure 6: Cross plots of 24 measured and calculated P-wave velocity samples versus permeability. The curves represent six flow units. The numbers in the plot are squirt-flow lengths in millimeters
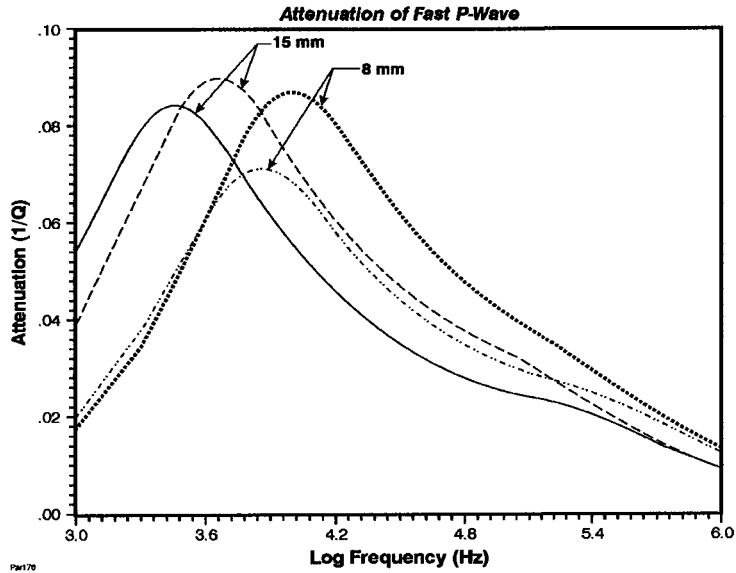
Figure 7: Attenuation curves of 4 samples. Response calculated for squirt-flow lengths of 8 and 15 mm
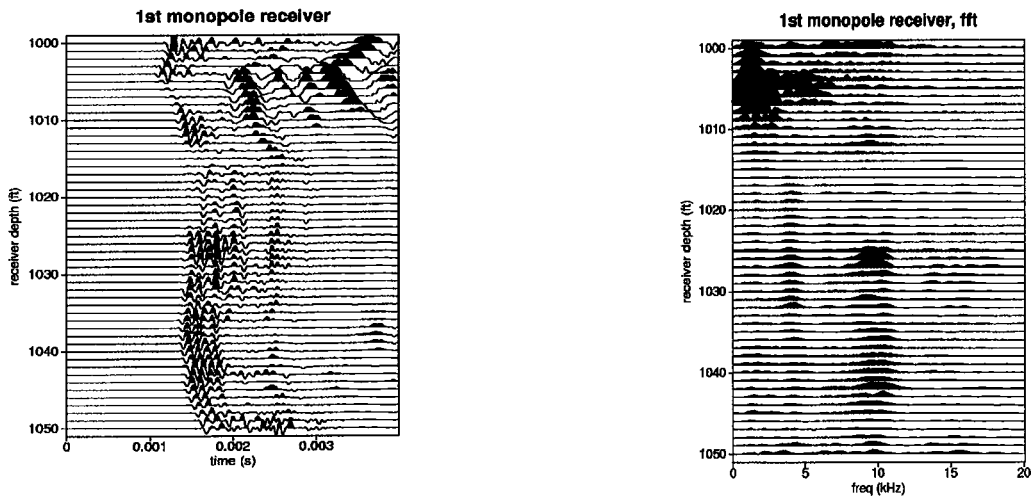

Figure 8: a) Full waveform sonic microseismogram, and b) its spectra from first receiver, showing data only between 1000 -1050 ft.